Determination of exchange energies in the sawtooth spin ring $\{Mo_{75}V_{20}\}$ by ESR

Yugo Oshima,[1,2,*] Hiroyuki Nojiri,[1,†] Jürgen Schnack,[3] Paul Kögerler,[4] and Marshall Luban[5]
[1]*Institute for Materials Research, Tohoku University, Katahira 2-1-1, Sendai 980-8577, Japan*
[2]*RIKEN, Wako, Saitama 351-0198, Japan*
[3]*Fakultät für Physik, Universität Bielefeld, Postfach 100131, D-33501 Bielefeld, Germany*
[4]*Institut für Anorganische Chemie, RWTH Aachen, Landoltweg 1, D-52074 Aachen, Germany*
[5]*Ames Laboratory and Department of Physics and Astronomy, Iowa State University, Ames, Iowa 50011, USA*
(Received 15 July 2011; revised manuscript received 27 November 2011; published 12 January 2012)

The magnetism of the polyoxometalate cluster $\{Mo_{75}V_{20}\}$, containing a sawtooth ring of 10 corner-sharing triangles located on the equator of the barrel-shaped molecule, has remained debatable since it is masked by contributions from impurities as well as temperature-independent paramagnetism. In this paper, we demonstrate the usefulness of electron spin resonance (ESR) measurements, since the temperature dependence of the ESR intensity can discriminate between impurity and molecular contributions. We determine the exchange parameters and therefore also the low-lying spectrum of $\{Mo_{75}V_{20}\}$, especially the low-lying singlet states which so far have been probed solely by specific-heat measurements.

DOI: 10.1103/PhysRevB.85.024413 PACS number(s): 75.10.Jm, 75.50.Xx, 75.40.Mg, 75.50.Ee

I. INTRODUCTION

The series of Keplerate molecules, $\{Mo_{72}Fe_{30}\}$, $\{Mo_{72}Cr_{30}\}$, $\{Mo_{72}V_{30}\}$, and $\{W_{72}V_{30}\}$, is one of the beautiful creations made possible by recent developments in modern chemistry.[1–10] In these nanosized molybdate or tungstate-based molecules, 30 magnetic ions are located on the 30 vertices of an icosidodecahedron and are antiferromagnetically coupled, resulting in triangular and pentagonal networks. As a result, this leads to a strongly frustrated cluster with a huge number of quantum states.[11] Since the number of states, $(2s+1)^{30}$, can be varied by substituting the magnetic ions [2^{30} and 6^{30} for V ($s = 1/2$) and Fe ($s = 5/2$), respectively], these are ideal systems for studying the transitions from quantum to classical behavior.

Among synthesized derivatives of the Keplerate clusters, the compound $\{Mo_{75}V_{20}\}$ is analogous to $\{Mo_{72}V_{30}\}$, except that the 10 V^{4+} ions ($s = 1/2$) located adjacent to the north and south poles of the icosidodecahedron are substituted by nonmagnetic ions.[12] Therefore, this compound is equivalent to a sawtooth chain of 10 triangles with a periodic boundary condition, as schematically shown in the inset of Fig. 1. Basically, $\{Mo_{75}V_{20}\}$ is classified as a sawtooth spin ring rather than a Keplerate cluster since it has only a partial substructure of $\{Mo_{72}V_{30}\}$. However, determining the exchange couplings of $\{Mo_{75}V_{20}\}$ can be a good reference for the characterization of its analogous compound $\{Mo_{72}V_{30}\}$. Moreover, sawtooth chains also belong to the class of frustrated antiferromagnetic spin systems with potentially very unusual magnetization curves,[13,14] as partly realized in the recently investigated magnetic material azurite.[15,16]

For $\{Mo_{75}V_{20}\}$, it turns out that the product χT of the magnetic susceptibility and temperature decreases steadily with decreasing temperature due to antiferromagnetic couplings, and it was assumed in Ref. 3 that the ground state is a singlet. Additionally, those authors estimated the exchange couplings between the magnetic ions from a theoretical fit to a reduced model that contains only a ring of six triangles. They concluded that their experimental results are well reproduced when $J_1 = 288$ K, $J_2 = 0.55 \cdot J_1$ (compare inset of Fig. 1), together with an additional coupling $J_3 = 0.20 \cdot J_1$ between the tips of every second triangle.[3]

Takemura and Fukumoto refined those parameters by using a finite-temperature Lanczos method for the full system of 10 coupled triangles.[17] They found similar exchange-coupling parameters, which are $J_1 = 388$ K, $J_2 = 0.42 \cdot J_1$, and $J_3 = 0.21 \cdot J_1$. However, these values are still under discussion for various reasons. The main concern is the unrealistically large exchange J_3, which should act across a distance of 11.7 Å, mediated by multicenter exchange pathways. Another problem is the fact that the susceptibility data are superimposed by an unknown amount of free vanadium ions (impurities) as well as by temperature-independent (i.e., van Vleck) paramagnetism typical of polyoxometalates.

We propose in this paper that electron spin resonance (ESR) is a unique method that overcomes these difficulties. It can separate the signals stemming from the intrinsic $\{Mo_{75}V_{20}\}$ and from impurities, since each ESR linewidth is qualitatively different. This enables us to obtain the pure magnetic response from $\{Mo_{75}V_{20}\}$, in contrast to the susceptibility measurements in which the intrinsic and extrinsic responses are mixed. Since the temperature dependence of the ESR intensity is related to the energies of the excited states, we are able to obtain information about the exchange couplings. The ratio of J_1 and J_2 determines the frustration of the sawtooth chain of which the density of low-lying singlet states is a fingerprint.[18,19] Usually the density of singlet levels is deduced from specific-heat measurements, but we will show below that ESR is also capable of determining the density of low-lying singlet states.

The paper is organized as follows. In Sec. II, we briefly explain the experimental method. Section III contains our experimental results that are compared to the calculated ESR intensities assuming various sets of model parameters. The paper closes with a short summary.

II. EXPERIMENT

The Terahertz Electron Spin Resonance Apparatus in the Institute for Materials Research (TESRA-IMR) of Tohoku

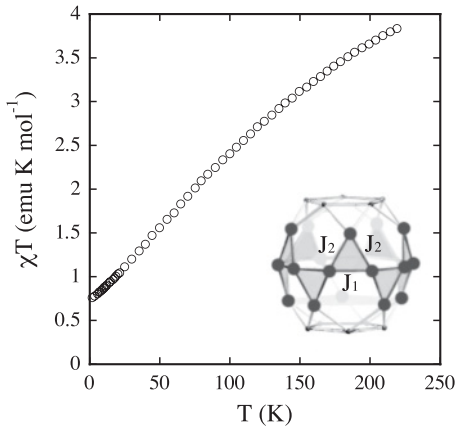

FIG. 1. Temperature dependence of χT from Ref. 3. The inset shows a scheme of the metal skeleton of $\{Mo_{75}V_{20}\}$ highlighting the nearest-neighbor exchange pattern between the V^{4+} ions.

University was used for the high-field ESR measurements.[20] A simple transmission method with a Faraday configuration was employed. We used conventional Gunn oscillators for the millimeter wave radiation, and an InSb detector for transmission detection. In addition, a pulsed magnetic field up to 8.5 T was generated from a 90 kJ capacitor bank. Two types of cryostats, a conventional ^{4}He-bath-type cryostat and gas-flow-type cryostat, were used for the measurements for the low- and high-temperature ranges, respectively. Powder samples were used in this study.

III. RESULTS AND DISCUSSION

A. High-field ESR results

Figure 2 shows the typical temperature dependence of the ESR spectra for $\{Mo_{75}V_{20}\}$. The employed frequency is 190 GHz, and the temperature is varied from 1.5 to 250 K. As shown in the inset of Fig. 2, two absorption lines, a shoulder and a sharp peak, which can be fitted with two separate lines,

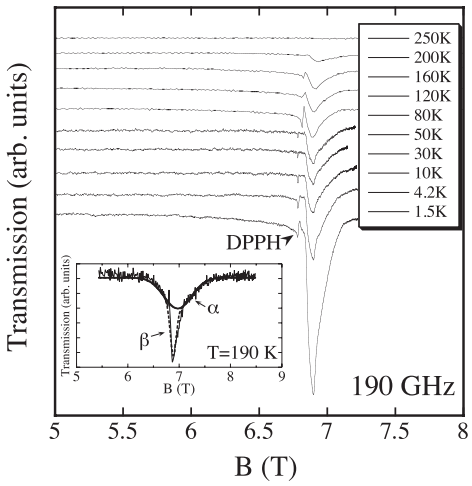

FIG. 2. Temperature dependence of ESR spectra for 190 GHz. The very narrow peak observed around 6.8 T is a field marker. The inset shows the spectrum for 190 K. The solid and dashed lines are fitting curves for resonance α and β, respectively (see text for details).

are observed at 190 K. Hereafter, we denote the observed resonances as α and β for the former and the latter, respectively. The tiny absorption observed at around 6.8 T is from DPPH, which stands for (2,2-diphenyl-1-picrylhydrazyl), and which is a field marker. The intensity of α gradually increases by decreasing the temperature, but quickly diminishes below 80 K, which is a typical ESR behavior of the excited states. On the other hand, the intensity of β is inversely proportional to the temperature, following Curie's law. Therefore, α can be assigned to the resonance originating from $\{Mo_{75}V_{20}\}$, and β from the impurities. The latter are vanadyl cations that are disordered over the cation sites. Since the synthesis needs an excess of vanadyl ions, some extra amount remains in the sample, which is rather common for these types of polyoxometalate clusters.[3] Since the singlet ground state is ESR silent, the absence of an intrinsic ESR signal from $\{Mo_{75}V_{20}\}$ at low temperature and the ESR observation of the excited states for relatively high temperatures suggests that the ground state of $\{Mo_{75}V_{20}\}$ is a singlet, which is consistent with magnetic susceptibility results.[3]

In the inset of Fig. 2, the absorption lines of α and β are fitted by Gaussian curves (solid and dashed curves, respectively), and integrated intensities for each temperature are obtained. The linewidths of the fitting curves can be found in the Supplemental Material.[25]

The integrated intensity of impurities (i.e., of resonance β), $I_{\rm imp}$, versus temperature is shown as solid circles in Fig. 3. According to the Boltzmann distribution, the ESR intensity of the $s = 1/2$ impurities can be written as

$$I_{\rm imp} = AN_{\rm imp}\tanh(\beta g\mu_B B/2)\,. \qquad (1)$$

Here A is a coefficient which is proportional to the power and frequency of the radiation, $N_{\rm imp}$ is the number of impurities,[21] and $\beta = 1/k_BT$ is the inverse temperature. g is the spectroscopic splitting factor and μ_B is the Bohr magneton.

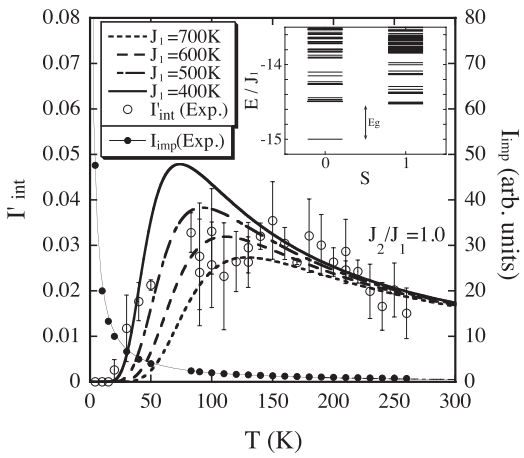

FIG. 3. Solid circles are the integrated intensities for resonance β coming from paramagnetic impurities; they are fitted using Eq. (1) (thin solid curve). Open circles are the normalized integrated intensities for resonance α coming from the intrinsic $\{Mo_{75}V_{20}\}$. Thick solid and dashed curves are calculated curves of the normalized integrated intensity for various values of J_1. The calculated curves are obtained from the singlet and triplet energy levels (inset), assuming an equilateral triangle model. The energy is normalized by J_1.

By using Eq. (1), $AN_{\rm imp} = 83.9 \pm 7.4$ is obtained from the fitting curve in Fig. 3 (thin solid curve).

On the other hand, the intrinsic ESR intensity of the excited triplet states, $I_{\rm int}$, which are the transitions $|M=-1\rangle \rightarrow |M=0\rangle$ and $|M=0\rangle \rightarrow |M=+1\rangle$, is proportional to the radiation coefficient A and the difference of the population between the transition levels, i.e.,

$$I_{\rm int} = A\{2(N_{\rm int,\,M=-1} - N_{\rm int,\,M=0}) + 2(N_{\rm int,\,M=0} - N_{\rm int,\,M=+1})\}. \tag{2}$$

The factor of 2 corresponds to the square of the transition matrix element.[21] When the intrinsic intensity $I_{\rm int}$ (i.e., intensity of α) is normalized by $AN_{\rm imp}$, which was already obtained above, the unknown radiation coefficient A can be eliminated, and then we obtain

$$I'_{\rm int} = \frac{N_{\rm int}}{N_{\rm imp}} \times \frac{2}{Z(T,B)} \times \sum_{\text{triplets } i} \{e^{-\beta(E_i - g\mu_B B)} - e^{-\beta(E_i + g\mu_B B)}\}, \tag{3}$$

where $Z(T,B)$ is the partition function,

$$Z(T,B) = \sum_{\text{singlets } k} e^{-\beta E_k} + \sum_{\text{triplets } i} \times \{e^{-\beta(E_i - g\mu_B B)} + e^{-\beta E_i} + e^{-\beta(E_i + g\mu_B B)}\}. \tag{4}$$

$N_{\rm int}$ is the number of $\{Mo_{75}V_{20}\}$, and E_k and E_i are the energies of the singlet and triplet states, respectively. The normalized values of $I'_{\rm int}$ are presented as open circles in Fig. 3. The error bars are obtained from the uncertainty of the fitting curves. Using Eq. (3), $I'_{\rm int}$ can be evaluated exactly using the energy levels of the singlet and triplet states, which can be obtained from the model Hamiltonian by diagonalization. This way the exchange constants can be determined by comparing experimental and theoretical values of $I'_{\rm int}$.

It is important to note that the whole procedure works with only singlet and triplet levels since the exchange constants are large and therefore states with $S \geqslant 2$ are irrelevant.

B. Theoretical models and analysis

The magnetism of $\{Mo_{75}V_{20}\}$ is modeled by a Heisenberg Hamiltonian augmented with a Zeeman term,

$$H = \sum_{i<j} J_{ij} \vec{\underset{\sim}{s}}_i \cdot \vec{\underset{\sim}{s}}_j + g\mu_B B \sum_j \underset{\sim}{s}^z_j. \tag{5}$$

Here J_{ij} is the exchange interaction between spins at sites i and j. The eigenvalues of this Hamiltonian can either be determined by complete matrix diagonalization or, for the low-lying levels, by the Lanczos method.[22–24] For our simulation, we considered the coupling J_1 on the equator and J_2 to the tips of the triangles, as schematically shown in the inset of Fig. 1. The low-energy part of the singlet and triplet sectors for $J_2 = J_1$ (i.e., equilateral triangle) is shown in the inset of Fig. 3. Note that energies are given as multiples of J_1. The lowest singlet level is degenerate due to the frustration of the triangular magnetic structure.[11]

From the energy eigenvalues, we can calculate $I'_{\rm int}$. The ratio $N_{\rm int}/N_{\rm imp} = 1/2$ is used since impurities of about $2\mu_B$ per molecular unit are observed in the magnetization measurements. It is also important to note that we have taken into account all singlet and triplet levels up to $10E_g$, where E_g is the gap between the ground state and the lowest triplet level (see inset of Fig. 3). In view of the experimental temperature range, this is more than sufficient since the exchange parameters turn out to be rather large.

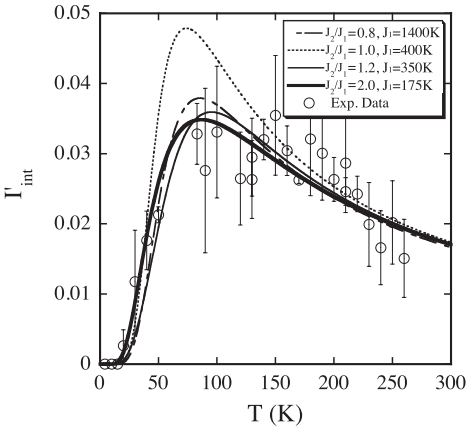

FIG. 4. Normalized integrated intensities for resonance α coming from the intrinsic $\{Mo_{75}V_{20}\}$ for various ratios J_2/J_1. The respective exchange parameters are shown in the legend.

The calculated $I'_{\rm int}$ curves for various $J_1 = J_2$ are shown in Fig. 3. The position of the maximum of the calculated curves changes by varying the exchange-coupling constant. The same holds true for the initial rise of the curve, which is related to the energy gap between the singlet and triplet states, i.e., E_g. On the other hand, the tail of $I'_{\rm int}$ turns out to be almost independent of the exchange parameter in the investigated range, which could possibly be discussed by looking at the high-temperature expansion.[26] For $J_1 = J_2 = 400$ K (thick solid curve in Fig. 3), the calculated curve fits well with the initial rising part and the tail part. However, a large difference is seen on the peak position. This suggests that an equilateral triangle model ($J_2 = J_1$) is not suited for this system, and that an isosceles triangle model ($J_2 \neq J_1$) should be considered.

Hence, we have investigated chains of isosceles triangles with various ratios J_2/J_1. Figure 4 shows the curves for $J_2/J_1 = 0.8, 1.0, 1.2$, and 2.0. The absolute values of the data are determined by the low-temperature behavior, i.e., the singlet-triplet gap, and the χ^2 parameter which gives a quantitative measure for the quality of the fitting curves.[27] The χ^2 parameters (lower is better) are 0.00055, 0.00132, 0.00044, and 0.00037 for $J_2/J_1 = 0.8, 1.0, 1.2$, and 2.0, respectively. It is obvious that a largely improved fit to our experimental data is provided by assuming the isosceles triangle model. The agreement in the observable $I'_{\rm int}$ appears to be better if $J_2 > J_1$. We emphasize that there is no need to introduce the additional exchange coupling J_3 between tips of neighboring triangles. This exchange is very unlikely anyway due to the very long exchange pathway.

In order to rationalize the differences between J_1 and J_2, it is helpful to look at the crystal structure of an individual triangle of $\{Mo_{75}V_{20}\}$, as schematically shown in Fig. 5. While the bonding length between vanadium atoms along J_1 and J_2 bonds does not vary much, the V-O-Mo bonding angles do.

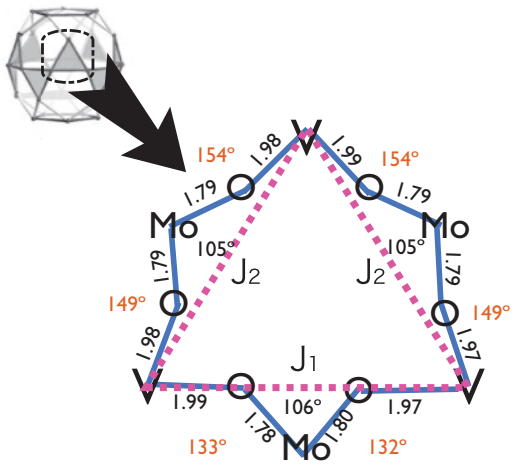

FIG. 5. (Color online) Bond lengths and angles for an individual triangle of $\{Mo_{75}V_{20}\}$.

Moreover, since the V-O-Mo bonding angles are larger along J_2 bonds, the Goodenough-Kanamori rule[28] suggests that the exchange should be stronger along this pathway, which is in accord with our observations. Among the two good fits, $J_2/J_1 = 1.2, J_1 = 350$ K and $J_2/J_1 = 2.0, J_1 = 175$ K, we tend to favor the second parameter set since this reproduces the low-temperature behavior much better. The absolute numbers are in good agreement with other polyoxometalates containing V^{4+} spin centers.[6,7,9]

Our results suggest that the type of frustration which is present in $\{Mo_{75}V_{20}\}$ is different from that in the original Keplerate molecules which are akin to the kagome lattice. Not only is $\{Mo_{75}V_{20}\}$ a quasi-one-dimensional object, but in addition the magnetic centers are not equivalent. The special ratio of $J_2/J_1 = 2.0$ relates it strongly to sawtooth chains with flat bands of one-magnon energies.[13,14] Such chains are characterized by giant magnetization steps of 50% of the saturation magnetization. Unfortunately, the exchange interactions present in $\{Mo_{75}V_{20}\}$ are much too large to observe such magnetization steps experimentally, even for the first one, let alone subsequent steps at larger fields.

IV. SUMMARY

In summary, we have performed ESR measurements of the polyoxometalate cluster $\{Mo_{75}V_{20}\}$. We succeeded in separating the intrinsic ESR signal of the molecules and the signal of the magnetic impurities. Via the temperature dependence of the integrated intensity, we could deduce the parameters of the underlying Heisenberg Hamiltonian. We also found that the additional exchange coupling J_3, which has been taken into account in previous studies,[3,17] is not necessary to explain the magnetic properties of $\{Mo_{75}V_{20}\}$.

Finally, we would like to stress that ESR is a powerful tool to study the low-energy spectrum, especially of frustrated magnetic systems. Since the sensitivity of ESR is very high, this method can in certain cases be far more effective than the specific-heat measurements in characterizing the low-lying density of states. This study shows only ESR results for a single frequency of 190 GHz. It is, of course, possible to obtain more detailed information on the spectrum by combining results using multiple frequencies.

ACKNOWLEDGMENTS

This work was supported by the Deutsche Forschungsgemeinschaft through the Research Unit 945. Ames Laboratory is operated for the US Department of Energy by Iowa State University under Contract No. W-7405-Eng-82. H.N. acknowledges the support by Grant-in-Aid for Scientific Research on Priority Areas (No. 13130204) and Scientific Research on Innovative Areas "Coordination Program" (No. 22108504) from MEXT, Japan and by the Shimazu Science Foundation. J.S. acknowledges the support from ICC-IMR.

*yugo@riken.jp
†nojiri@imr.tohoku.ac.jp

[1] A. Müller, F. Peters, M. Pope, and D. Gatteschi, Chem. Rev. **98**, 239 (1998).
[2] A. Müller, S. Sarkar, S. Q. N. Shah, H. Bögge, M. Schmidtmann, S. Sarkar, P. Kögerler, B. Hauptfleisch, A. Trautwein, and V. Schünemann, Angew. Chem. Int. Ed. **38**, 3238 (1999).
[3] A. Müller, P. Kögerler, and A. Dress, Coord. Chem. Rev. **222**, 193 (2001).
[4] A. Müller, M. Luban, C. Schröder, R. Modler, P. Kögerler, M. Axenovich, J. Schnack, P. C. Canfield, S. Bud'ko, and N. Harrison, ChemPhysChem. **2**, 517 (2001).
[5] A. Müller, P. Kögerler, and C. Kuhlmann, Chem. Commun. 1347 (1999).
[6] A. Müller, A. M. Todea, J. van Slageren, M. Dressel, H. Bögge, M. Schmidtmann, M. Luban, L. Engelhardt, and M. Rusu, Angew. Chem. Int. Ed. **44**, 3857 (2005).
[7] B. Botar, P. Kögerler, and C. L. Hill, Chem. Commun. 3138 (2005).
[8] U. Kortz, A. Müller, J. van Slageren, J. Schnack, N. S. Dalal, and M. Dressel, Coord. Chem. Rev. **253**, 2315 (2009).
[9] A. M. Todea, A. Merca, H. Bögge, T. Glaser, L. Engelhardt, R. Prozorov, M. Luban, and A. Müller, Chem. Commun. 3351 (2009).
[10] P. Kögerler, B. Tsukerblat, and A. Müller, Dalton Trans. **39**, 21 (2010).
[11] J. Schnack, Dalton Trans. **39**, 4677 (2010).
[12] A. Müller, M. Koop, H. Bögge, M. Schmidtmann, F. Peters, and P. Kögerler, Chem. Commun. 1885 (1999).
[13] J. Schulenburg, A. Honecker, J. Schnack, J. Richter, and H.-J. Schmidt, Phys. Rev. Lett. **88**, 167207 (2002).
[14] J. Richter, J. Schulenburg, A. Honecker, J. Schnack, and H.-J. Schmidt, J. Phys. Condens. Matter **16**, S779 (2004).

[15]K. C. Rule, A. U. B. Wolter, S. Süllow, D. A. Tennant, A. Brühl, S. Köhler, B. Wolf, M. Lang, and J. Schreuer, Phys. Rev. Lett. **100**, 117202 (2008).
[16]A. Honecker, S. Hu, R. Peters, and J. Richter, J. Phys. Condens. Matter **23**, 164211 (2011).
[17]S. Takemura and Y. Fukumoto, J. Phys. Soc. Jpn. **76**, 083709 (2007).
[18]C. Waldtmann, H. U. Everts, B. Bernu, C. Lhuillier, P. Sindzingre, P. Lecheminant, and L. Pierre, Eur. Phys. J. B **2**, 501 (1998).
[19]E. Berg, E. Altman, and A. Auerbach, Phys. Rev. Lett. **90**, 147204 (2003).
[20]H. Nojiri, Y. Ajiro, T. Asano, and J.-P. Boucher, New J. Phys. **8**, 218 (2006).
[21]A. Abragam and B. Bleaney, *Electron Paramagnetic Resonance of Transition Ions* (Dover, New York, 1986), p. 119.
[22]C. Lanczos, J. Res. Natl. Bur. Stand. **45**, 255 (1950).
[23]J. Schnack, P. Hage, and H.-J. Schmidt, J. Comput. Phys. **227**, 4512 (2008).
[24]R. Schnalle and J. Schnack, Int. Rev. Phys. Chem. **29**, 403 (2010).
[25]See Supplemental Material at http://link.aps.org/supplemental/10.1103/PhysRevB.85.024413 for the temperature dependence of the linewidth.
[26]H.-J. Schmidt, J. Schnack, and M. Luban, Phys. Rev. B **64**, 224415 (2001).
[27]W. H. Press, B. P. Flannery, S. A. Teukolsky, and W. T. Vetterling, *Numerical Recipes in C: The Art of Scientific Computing* (Cambridge University Press, Cambridge, 1988).
[28]J. B. Goodenough, Phys. Rev. **100**, 564 (1955).